Soft Matter

PAPER

View Article Online
View Journal | View Issue

Cite this: *Soft Matter*, 2022, **18**, 7604

Magnetic vitrimer-based soft robotics†

Gaoweiang Dong,[a] Qiguang He[b] and Shengqiang Cai *[a]

Magnetically responsive elastomers, consisting of elastomer embedded with magnetic particles, can produce fast and reversible actuation when subjected to a magnetic field. They have been extensively explored to construct versatile remotely controllable soft robots. Nevertheless, the magnetically induced actuation strain in elastomers is typically small, which limits its broad applications. Recently, magnetic particles have been mixed with viscous fluids to enable giant magnetically induced deformations. However, their response speed is slow and the actuation is usually irreversible. In this work, we have developed a magnetic vitrimer (MV), with magnetic particles mixed with the polymer network containing abundant dynamic covalent bonds. At room temperature, the MV behaves like a regular magnetically responsive elastomer. When the temperature is elevated to the exchange reaction temperature of the dynamic covalent bonds, the material behaves like a viscous magnetically responsive fluid, which can produce large deformations. The embedded magnetic particles and the vitrimer matrix also make the material self-healable without requiring any direct touch. We have demonstrated that with the guidance of an externally applied magnetic field, a MV-based soft robot can pass through a confined space, dramatically change its configuration, self-heal without any contact, catch, secure and release a fast-moving object, and move along a planned path.

Received 1st July 2022,
Accepted 10th September 2022

DOI: 10.1039/d2sm00893a

rsc.li/soft-matter-journal

1. Introduction

Shape-morphing materials that can alter their configurations under various external stimuli, such as temperature, light, pH, humidity, and electrical and magnetic fields, have been explored for diverse applications such as actuators, wearable devices, soft robotics and flexible electronics.[1] In this context, various stimuli-responsive materials have been developed, including liquid crystal elastomers,[2] stimuli-responsive hydrogels[3] and shape memory polymers.[4] In particular, magnetically responsive soft materials composed of magnetic particles and polymer matrix have shown many unique and desirable features including fast response,[5] reversible actuation,[6] self-healing[7] and facile controllability,[8] which has great potential in various applications with minimally invasive interactions.[9,10]

Commonly adopted actuation mechanisms of magnetically responsive soft composite materials rely on the magnetic gradient-induced external force and magnetic field-induced torque exerted on the materials.[11] When the magnetic particles are embedded into a matrix, an external magnetic field can be used to remotely and rapidly actuate the soft composite. Recent studies have demonstrated several creative applications utilizing these composites. For example, a magnetically actuated soft continuum robot has been controlled to actively navigate and steer in confined environments.[8] Hu *et al.*[6] developed a small-scale magnetoelastic soft robot with a silicone elastomer matrix (Ecoflex 00-10) embedded with hard magnetic neodymium-iron-boron (NdFeB) microparticles, which exhibited enhanced mobility and multimodal locomotion with a controlled external magnetic field and carefully designed magnetic domains in the composite. Moreover, Kim *et al.*[5] fabricated a magnetic responsive elastomer through a 3D printing technique, enabling fast transformations between complex 3D shapes by programming ferromagnetic domains. For the examples above, elastic actuation of the polymer matrix is employed, where the material returns to its original configuration upon the removal of the magnetic field.

Limited actuation modes and deformability of elastomer-based soft actuators can be improved by substituting the elastomer matrix with viscous fluid. Viscous fluid greatly enhances the deformability of the soft actuators. Recent studies have reported the use of fluid-based magnetic responsive actuators such as ferrofluids[12] and magnetic slime[13] to build non-invasive and reconfigurable miniature robots, which show nearly infinite deformability.[14] Thanks to the flowability of the viscous fluid, these soft actuators are capable of passing through confined spaces that are much smaller than their sizes

[a] *Department of Mechanical and Aerospace Engineering, University of California, San Diego, La Jolla, CA 92093, USA. E-mail: shqcai@ucsd.edu*
[b] *Mechanical Engineering and Applied Mechanics Department, University of Pennsylvania, Philadelphia, 19104, USA*

† Electronic supplementary information (ESI) available: Videos corresponding to Fig. 4 and 6. See DOI: https://doi.org/10.1039/d2sm00893a

without any damage. Moreover, fluid-based magnetic robots can generate drastic shape changes under magnetic control, enabling novel functionalities including object manipulation and transportation.[15–19] For instance, Fan *et al.*[16] have developed collective magnetically actuated ferrofluid with multiple deformation modes such as splitting and forming of various liquid-robot aggregates, which can be utilized for navigation in multi-terrain surfaces and confined spaces. Researchers have also investigated a single ferrofluid droplet controlled by spatiotemporally changing the external magnetic field to deliver and manipulate delicate objects.[20] However, magnetically actuated tiny droplets often experience additional resistance from their surface tension. One recent work[13] has proposed magnetic slime as a magnetic actuated soft robot with great adaptability and deformability compared with the conventional magnetic droplet robot, being able to work across multiple interfaces and underwater. However, those soft actuators usually do not show a reversible and elastic response, which are often needed for many tasks such as cyclic gripping and releasing items, reversible expansion/collapsing and impulsive motion based on the spring-latch mechanism.

The elastomer-based and fluid-based magnetic soft actuators both have been studied extensively, but each type has certain limitations: the actuation strain of elastomer-based magnetic actuators is typically small, while the actuation of most fluid-based magnetic actuators is irreversible. To combine the characteristics of both elastomer-based actuators and fluid-based actuators, researchers have employed the polymer matrix with dynamic covalent bonds, which can rearrange their network under certain stimuli such as heat and ultraviolet (UV) irradiation.[9,21,22] Kuang *et al.*[23] have recently developed polymers with dynamic covalent bonds embedded with hard-magnetic particles for modular assembling and reconfigurable architectures with reprogrammable actuation modes. However, versatile and drastic permanent shape morphing have not yet been demonstrated.

In this work, we have developed a magnetically responsive soft composite with a polymer matrix containing disulfide bonds embedded with magnetic particles. The exchange reaction of disulfide bonds occurs under heat or infrared (IR) irradiation. Consequently, disulfide bonds dynamically rearrange and the mobility of the polymer chains significantly increases.[24,25] The deformation mechanism of the magnetic vitrimer (MV) lies in its temperature-sensitive rheological behavior, which allows reversible actuation at room temperature and also drastic shape change with a mild temperature increase. Besides, we used a laser to remotely control the local temperature field of the MV to enable local and more precise shape morphing. Furthermore, unlike most self-healing materials that need to be manually brought together[7] and subjected to mechanical pressure[25] during the healing process, a broken MV can self-heal without being touched under the guidance of an external magnetic field. As shown in Fig. 1, we demonstrated an MV-based soft robot that can: (1) pass through a gap that is smaller than its original size, (2) dramatically transform its shape into a soft robotic gripper, (3) self-heal without contact from permanent damage, (4) catch and secure a fast-moving object, and (5) transport and release the object.

2. Results and discussion

2.1. Fabrication and characterization of the MV

The schematics of the material preparation are shown in Fig. 2A and B: we prepared the MV using epoxy monomers (EPS25, epoxy equivalent = 462 g equiv.$^{-1}$) with stoichiometric mixtures of two sulfhydryls: 2,2′-(ethylenedioxy)diethanethiol (EDDET) and pentaerythritol tetrakis (3-mercaptopropionate) (PETMP). The polymer network is formed through the thiol–epoxy reaction, where EDDET with two thiol groups forms the polymer chains together with EPS25 and PETMP with four thiol groups crosslinks the polymer chains into a network. We chose (dimethylamino)pyridine (DMAP) as the catalyst. In addition, we tuned the molar

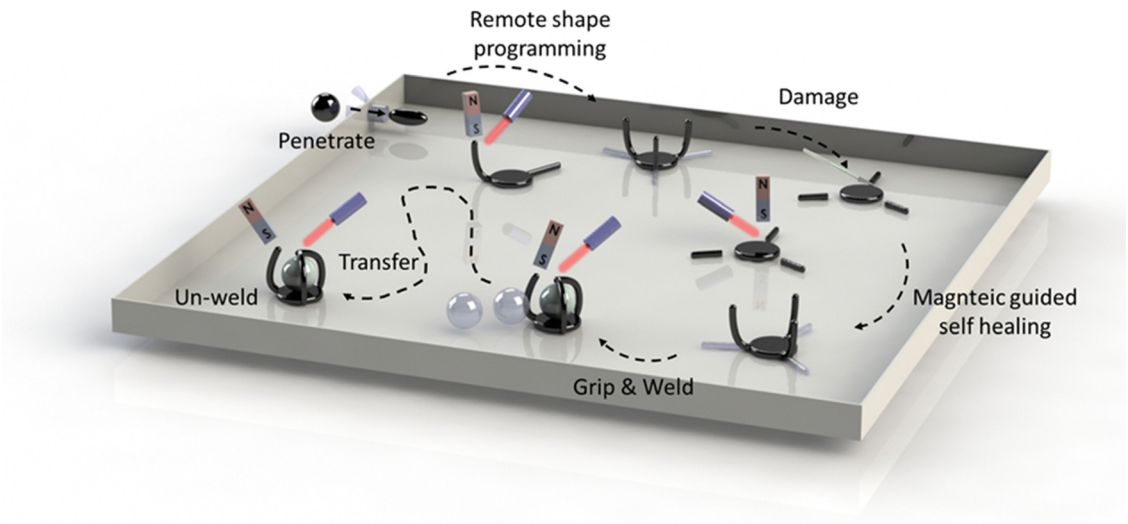

Fig. 1 A magnetic vitrimer-based soft robot can squeeze itself to pass through an extremely confined space, reshape, self-heal, grip, transport and release an object.

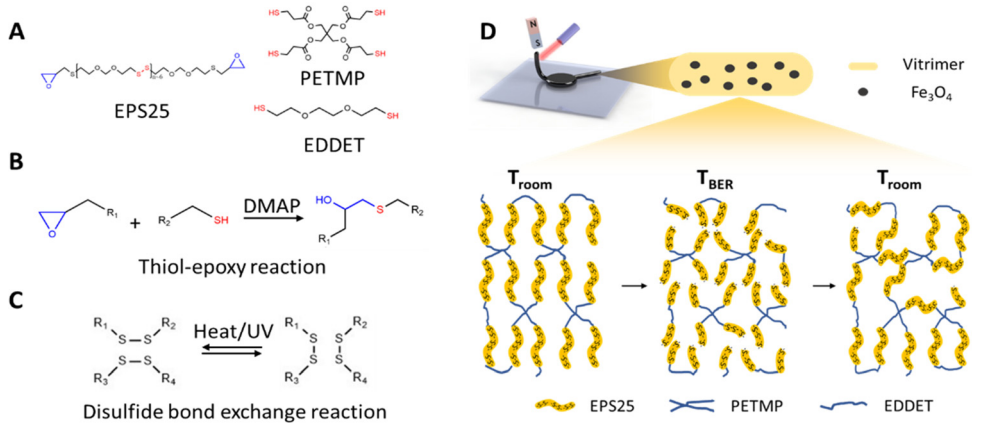

Fig. 2 Preparation and the molecular structure of the magnetic vitrimer used in the current study. (A) Molecular structure of the monomer EPS25, crosslinker PETMP and chain extender EDDET. (B) Crosslinking mechanism of the thiol–epoxy reaction with DMAP (4-dimethylaaminopyridine) as the catalyst. (C) Mechanism of the disulfide bond exchange reaction. (D) Reconfiguration mechanism of the magnetic vitrimer.

ratio (γ) of thiol groups from EDDET and PETMP to tailor the crosslinking density of the MV and thus its thermomechanical properties, while maintaining the thiol group concentration the same. As shown in Fig. 2C, as the temperature rises, the disulfide bonds can readily be cleaved and re-formed by a reduction reaction and an oxidation reaction, respectively,[24,26] endowing the fluid-like behavior to the vitrimer.

To prepare a magnetically responsive vitrimer, we embedded magnetic microparticles (Fe_3O_4) into the polymer matrix, where the schematic of the MV and its reconfiguration mechanism are illustrated in Fig. 2D. The monomers consist of abundant disulfide bonds and the bond exchange reaction (BER) becomes more active at an elevated temperature (T_{BER}), leading to increased flowability of the composite. As a result, a magnetic gradient can induce dramatic and irreversible shape change of magnetic vitrimer in a controlled manner. When the environmental temperature is decreased to room temperature, the disulfide bond exchange reaction becomes much less active and the MV behaves like a normal elastomer. The temperature dependent behavior of the MV allows its shape reprogrammability and also reversible actuation.

To evaluate the potential of using MV for soft robotics, we systematically studied the effects of the two major parameters on the thermomechanical properties of the material: the stoichiometric ratio γ of the chain extender to the crosslinker and the weight percentage of the magnetic particles in the composite. We varied the γ value from 0 to 1 to investigate the effect of the crosslinking density on the properties of the MV composite at an ambient temperature (30 °C) with a fixed magnetic particle loading (10 wt%). Among all the samples, we fixed the ratio between thiol groups (from EDDET and PETMP) and epoxy groups (from EPS25) to keep the concentration of the dynamic covalent bond constant. As illustrated in Fig. 3A (G_R is the relaxation shear modulus), the normalized stress relaxation for the samples with different γ values shows a similar relaxation time, suggesting that the kinetics of the disulfide bond exchange reaction is not affected by the crosslinking density. However, the magnitude of the relaxation modulus is negatively correlated to γ. The stress *vs.* strain curves shown in Fig. 3B show that both stiffness and strength of the MV increase as the γ value decreases. The γ value is the molar ratio of the thiol group from EDDET and PETMP, where PETMP has four thiol groups and forms a crosslinking junction. Therefore, the material modulus and strength increase by increasing the crosslinking density.

In addition to the γ value, the magnetic particle loading also affects the mechanical behavior of MV. In Fig. 3C and D, as the loading of magnetic particles increases from 0 wt% to 20 wt% for a given γ value (0.5), the relaxation time of the material increases by one order of magnitude and the material strength doubles. Both the mechanical properties and magnetic response of the MV vary with the concentration of magnetic particles. Although higher magnetic particle concentration can enhance magnetic response, introducing too many magnetic particles to the vitrimer matrix can affect the viscoelastic properties of MV. Fig. S1 (ESI†) shows that the viscosity of MV increases with increasing concentration of magnetic particles. Therefore, at ambient temperature, higher magnetic particle loading increases the stiffness of the MV, requiring larger force to actuate the body, which limits the magnetic actuation capabilities of the material. Moreover, at high temperatures, the viscosity will also increase with higher magnetic particle loading, which limits the flowability of the MV.

In the context of soft robotic grippers, their primary functionality is the ability to grasp or catch an object and hold against the external disturbance, and high compliance of the material can reduce control complexity. In most applications, the time scale of grasping or catching an object is typically less than a few seconds,[27–29] indicating that the relaxation time of the composite at room temperature is longer than tens of seconds. On the other hand, the low viscosity of MV at high temperatures is desired during shape morphing. Therefore, we chose the molar ratio (γ = 0.5) and magnetic particle loading (= 10 wt%) to prepare the MV for the rest of this study, with a relaxation time of around 100 seconds and a secant modulus of 0.11 MPa at ambient temperature (Fig. S2, ESI†). As shown in Fig. 3E, using the selected MV, we conducted the stress

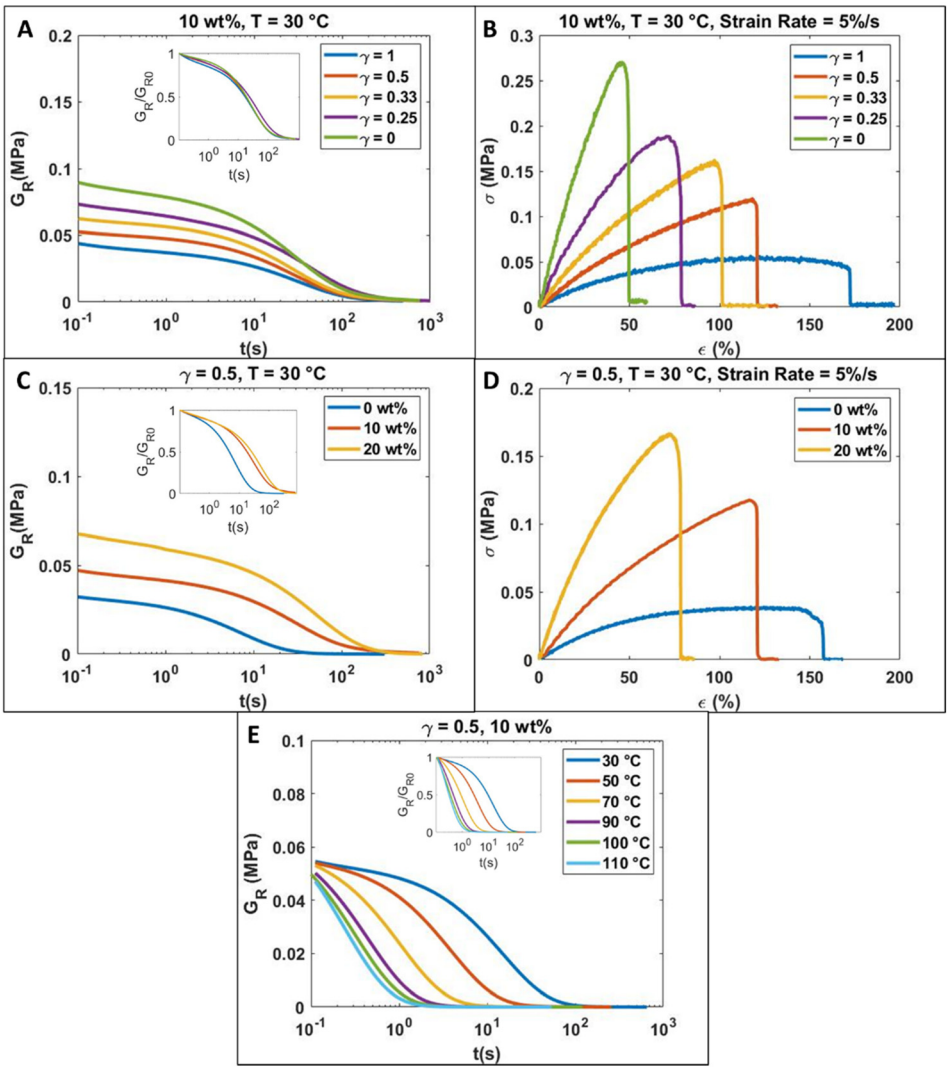

Fig. 3 Thermomechanical characterizations of the MVs. (A) Stress relaxation of MVs with different chain extender-crosslinker ratios (γ) at T = 30 °C. The inset shows the normalized experimental results. (B) Uniaxial tensile testing results of MVs with different chain extender-crosslinker ratios (γ) at T = 30 °C. (C) Stress relaxation of MVs with different weight percent of magnetic particles at T = 30 °C and the inset shows the normalized results. (D) Uniaxial tensile testing results of MV with different weight percentages of magnetic particles at T = 30 °C. (E) Stress relaxation of MVs at different temperatures.

relaxation tests at different temperatures. The decrease of the relaxation time with increasing temperature is due to the accelerated disulfide bond exchange reaction at higher temperatures.[30]

Finally, we also examined the possible degradation of the properties of the MV during its storage. Fig. S3 (ESI†) shows that as the storage time increases, the storage modulus (G') increases and tan(δ) decreases. Such degradation property is mainly due to the decrease of the efficiency of the catalyst (DMAP) over time in the system.[31,32] It is noted that there have been various types of vitrimers, the dynamic bond exchanging reaction of which does not need any catalyst.[33] The properties of those vitrimers are often more stable after a long period of storage.

2.2. Demonstration of MV-based soft robotics

In this study, we demonstrated four distinct working modes of an MV-based soft robot: (1) passing through confined environments, (2) permanent shape morphing with remote control, (3) touchless self-healing and (4) manipulating objects as a soft gripper.

We first demonstrated the heat-enhanced flowability of MV as shown in Fig. 4A and Video 1, ESI.† A spherical MV was blocked by a narrow opening. The external magnetic field could not drive the MV to move through the opening at room temperature because of its relatively high stiffness. When we heated the local environment to 100 °C, the disulfide bond exchange reaction became more active, leading to a significant increase of the flowability of the MV. With an applied magnetic field, the magnetic gradient-induced pulling force exerted on the MV drove it to flow through the narrow opening within around 1 min. The dimensions of the MV before and after penetrating through the small opening are shown in Fig. S4, ESI.† The magnetic field gradient for actuation was generated by a cubic permanent magnet (25 × 25 × 25 mm, N52 Neodymium Magnet from KJ Magnetics), which has a magnetic

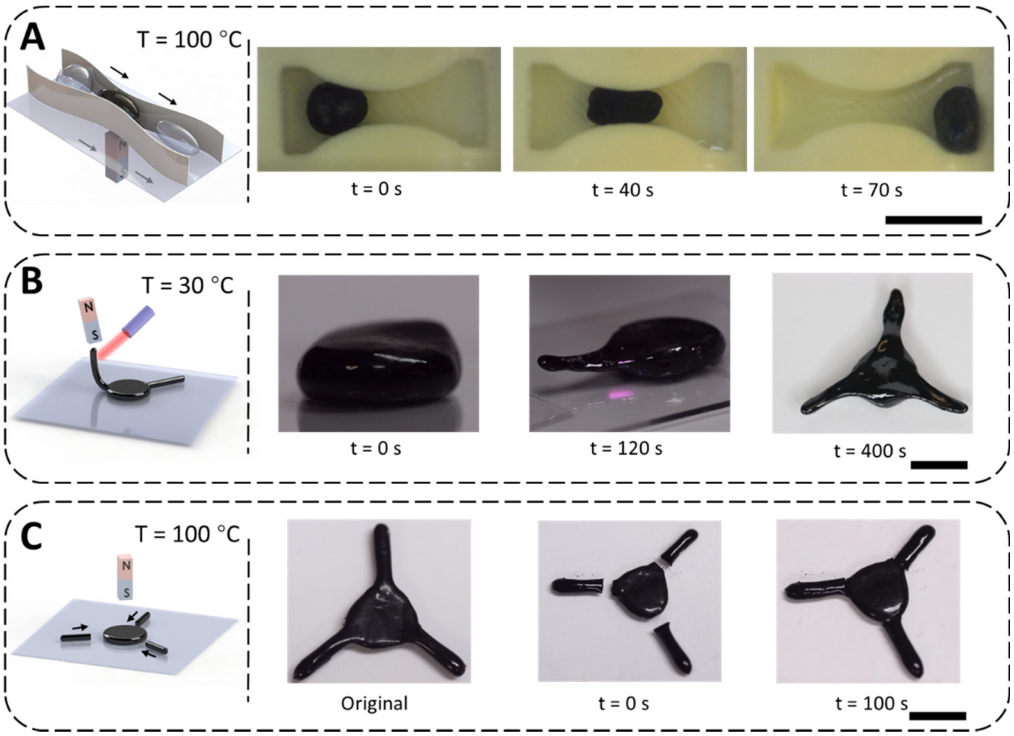

Fig. 4 Heat enabled flowability, remote shape morphing and self-healing of MV. (A) At an elevated temperature (100 °C), an MV sphere can pass through a narrow opening with an applied magnetic field. Scale bar, 1 cm. (B) An MV disk can transform into a soft gripper by applying local heating with a laser beam and a magnetic field by a permanent magnet. Scale bar, 1 cm. (C) Self-healing capability of the soft gripper after severe damage. Scale bar, 1 cm.

field density of 4000 Gauss at the surface, measured by a hand-held Gauss meter (TD8620, Tunkia). The MV was able to flow through the opening at a distance around 10–20 mm away from the surface of the magnet, where the magnetic field density ranges from 1500 to 500 Gauss. After the MV robot completely went through the opening, both the thermal and magnetic fields were removed, and the material regained its elasticity.

We further extended the working mechanism of the MV to broaden its functionality by introducing localized heating, which can enhance the flowability of specific regions in the material. With the application of magnetic gradient, remote control of shape morphing could be realized in a designed fashion. As shown in Fig. 4B, with the assistance of the local thermal field generated by an infrared laser pointer (Sky laser, PL-808-1000B) and the magnetic gradient in-line with the direction of robotic gripper 'arms', the MV could change its configuration from a disk shape to a soft robotic gripper.

We next demonstrated the magnetically guided self-healing of the MV gripper. As shown in Fig. 4C and Video 2 (ESI†), the three 'arms' of the MV gripper were separated from the 'body' by a sharp blade. To initiate the self-healing process, we placed a permanent magnet on the top of the gripper and heated up the environment to 100 °C for 100 seconds. The magnetic gradient-induced pulling force allowed the broken 'arms' to move toward the main 'body' without direct applied contact. The elevated temperature accelerated the disulfide bond exchange reaction, permitting the self-healing of the MV gripper in the broken regions. Upon the removal of the magnetic and thermal field, the gripper regained its integrity and elasticity.

To further investigate the self-healing efficiency of MV, we studied the self-healing time of MV by conducting the tensile tests. As illustrated in Fig. 5A, the specimens were cut into two halves at ambient temperature (30 °C) using a sharp blade. The two segments were then brought into contact with the help of an external magnetic field and put at 100 °C for various time periods. The self-healing times for the MV sample were set to 0, 10, 30, 60, 120, 200, 300, 600 and 900 seconds. We conducted the tensile test at 5% s^{-1} strain rate and the results are shown in Fig. 5B. Self-healed MVs exhibited similar strength at 120, 200, 300, 600 and 900 seconds at around 0.8 MPa, which was around 80% of the pristine sample. The results also agreed with our previous measurements of the relaxation time, which was around 100 seconds, indicating that the dynamic bonds need around 100 seconds to form between separated pieces.

Finally, we demonstrated the capability of the soft robotic gripper to interact with a moving object through magnetic control. As shown in Fig. 6A, a magnetic field with a strong gradient exerted a pulling force on the iron oxide microparticles, which could attract each 'arm' to align with the magnetic field. On the other hand, the 'arm' also tended to align with the magnetic field direction, due to the body-force torque from anisotropic gripper geometry and paramagnetic torque from iron oxide anisotropic distribution. Therefore, the deformation resulted from a balance between the elastic restoring force of the gripper and magnetic force exerted onto the gripper. As shown in

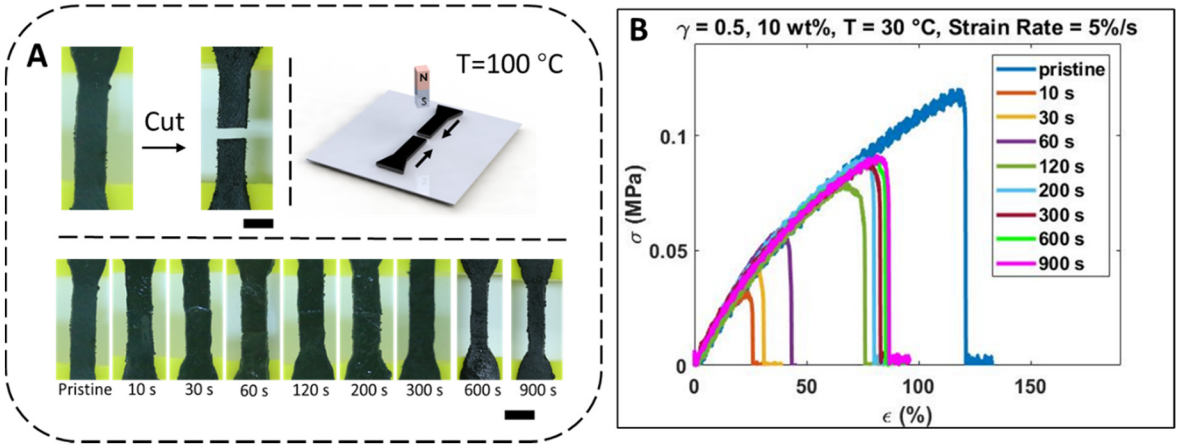

Fig. 5 Magnetically assisted self-healing of MV. (A) MV strips were first cut into two parts at 30 °C. Then, assisted by the external magnetic field, the two broken parts were brought into contact and heated up at a temperature of 100 °C to trigger the dynamic bond exchange reaction. Specimens were healed for different time periods. Scale bar, 2 mm. (B) Tensile stress–strain relationship of self-healed MV strips with different healing times.

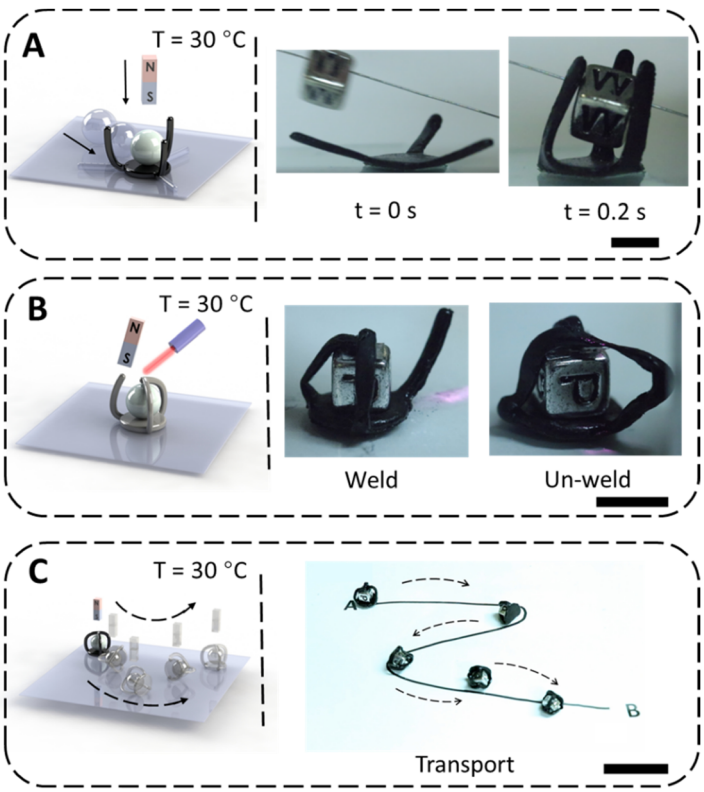

Fig. 6 MV-based soft gripper. (A) The soft robotic gripper can catch a moving object through fast actuation. Scale bar, 1 cm. (B) Welding/un-welding of the gripper to secure/release the object. Scale bar, 1 cm. (C) With an externally applied magnetic field, the soft robotic gripper can carry the object and move along a planned path. Scale bar, 5 cm.

Video 3 (ESI†), at the ambient temperature (T = 30 °C), a fast response of the gripper controlled by a permanent magnet allowed the soft robotic gripper to catch a fast-moving object. The gripper was also able to release the object on demand. By further harnessing the remote local shape morphing capability of MV, the soft robotic gripper could secure and release the object by 'welding' and 'un-welding' of the 'arms', as shown in Fig. 6B and Video 4, ESI.† With careful manipulation of a magnet and a local thermal field, the tip of the 'arms' could be connected or disconnected with an object held inside. In Fig. 6C, the welded soft robotic gripper was able to carry the object and travel along a planned route under the guidance of a magnetic field. Moreover, the soft robotic gripper could protect the object from possible mechanical damage, due to the viscoelastic nature of MV.

3. Experimental methods

3.1. Magnetic vitrimer preparation

MV was prepared by cross-linking the epoxy monomer with 2 different sulfhydryls. Briefly, the monomer EPS25 (ThioPlast, epoxy equivalent = 462 g equiv.$^{-1}$, kindly provided by Norton Functional Chemicals GmbH) and a stoichiometric mixture (γ = 0.5) of two crosslinkers: 2,2′-(ethylenedioxy)diethanethiol (EDDET, >95%, Sigma Aldrich) and pentaerythritol tetrakis (3-mercaptopropionate) (PETMP, >95%, Sigma Aldrich) were manually mixed at room temperature. Then, 1 wt% 4-DMAP (>99.0%, Sigma Aldrich) and 10 wt% of iron oxide microparticles (Fe_3O_4, >98%, $d \sim 1$ μm, Alpha Chemicals) were manually added and mixed into the composition to obtain a homogeneous blend, which was confirmed by the optical microscopic images in Fig. S5 (ESI†). Finally, the mixture was poured into a glass Petri dish and cured at 60 °C for 3 hours. As shown in Fig. S6 (ESI†), the storage modulus (G') and loss modulus (G'') of MV change little after 3 hours of curing, indicating that MV is fully cured. To obtain an MV sheet with the desired thickness for characterization purposes, the samples and a spacer were hot-pressed using a heat press machine (Carver, Wabash) at 100 °C for 2 minutes between parchment paper. All samples were cooled to room temperature and stored at 30 °C for 24 hours before characterization.

3.2. Characterization

The uniaxial test was performed on a dynamic mechanical analysis equipment RSA-G2 (TA instruments, New Castle) using dog bone samples (effective dimension: 2 × 20 × 0.8 mm). The strain rate was 5% s^{-1}. For each sample, three specimens were tested and the average results were reported. The stress relaxation test was conducted on a rheometer DHR3 (TA Instruments, New Castle) using disc samples (diameter: 20 mm, thickness: 0.8 mm). The samples were equilibrated at a specified temperature for 5 minutes, and then a constant shear strain of 30% (0.015 rad) was applied to monitor the evolution of stress as a function of time. The homogeneous thermal field was created within an in-house built heating chamber including 4 polyimide heating pads (5 V, 1 W, 30 × 40 mm) with a uniform thermal field of up to 130 °C. The local thermal field was generated with an infra-red laser pointer PL-808-2000 (Sky Laser, 2 W). The videos and pictures were captured using a digital camera (Cannon EOS 80D).

Conclusion

In this article, we have designed and fabricated magnetic vitrimer-based soft robots. The exchange reaction activity of the dynamic bonds within the MV increases at an elevated temperature, allowing the MV soft robots to have dramatic and irreversible shape change with the applied magnetic field. Such a dramatic shape change enables the MV-based soft robot to pass through a significantly confined space. With the laser-induced local heating and external magnetic field, the MV-based soft robot can also change its shape with respect to the control. Moreover, the combination of embedded magnetic particles and exchange reaction of the dynamic bond in the MV makes it self-healable without requiring any direct touch. At room temperature, MV behaves like a regular elastomer, and the MV-based soft robotic gripper can achieve fast catching, releasing and locomotion.

Conflicts of interest

There are no conflicts to declare.

Acknowledgements

This work was supported by the US Army Research Office (Grant No. W911NF-20-2-0182).

References

1 J. Shintake, V. Cacucciolo, D. Floreano and H. Shea, Soft Robotic Grippers, *Adv. Mater.*, 2018, **30**(29), 1707035, DOI: 10.1002/adma.201707035.
2 Q. He, Z. Wang, Y. Wang, Z. Song and S. Cai, Recyclable and Self-Repairable Fluid-Driven Liquid Crystal Elastomer Actuator, *ACS Appl. Mater. Interfaces*, 2020, **12**(31), 35464–35474, DOI: 10.1021/acsami.0c10021.
3 L. Ionov, Hydrogel-Based Actuators: Possibilities and Limitations, *Mater. Today*, 2014, **17**(10), 494–503, DOI: 10.1016/j.mattod.2014.07.002.
4 H. Meng and G. Li, A Review of Stimuli-Responsive Shape Memory Polymer Composites, *Polymer*, 2013, **54**(9), 2199–2221, DOI: 10.1016/j.polymer.2013.02.023.
5 Y. Kim, H. Yuk, R. Zhao, S. A. Chester and X. Zhao, Printing Ferromagnetic Domains for Untethered Fast-Transforming Soft Materials, *Nature*, 2018, **558**(7709), 274–279, DOI: 10.1038/s41586-018-0185-0.
6 W. Hu, G. Z. Lum, M. Mastrangeli and M. Sitti, Small-Scale Soft-Bodied Robot with Multimodal Locomotion, *Nature*, 2018, **554**(7690), 81–85, DOI: 10.1038/nature25443.
7 E. Ogliani, L. Yu, I. Javakhishvili and A. L. Skov, A Thermo-Reversible Silicone Elastomer with Remotely Controlled Self-Healing, *RSC Adv.*, 2018, **8**(15), 8285–8291, DOI: 10.1039/C7RA13686B.
8 Y. Kim, G. A. Parada, S. Liu and X. Zhao, Ferromagnetic Soft Continuum Robots, *Sci. Rob.*, 2019, **4**(33), eaax7329, DOI: 10.1126/scirobotics.aax7329.
9 Y. Cheng, K. H. Chan, X.-Q. Wang, T. Ding, T. Li, C. Zhang, W. Lu, Y. Zhou and G. W. Ho, A Fast Autonomous Healing Magnetic Elastomer for Instantly Recoverable, Modularly Programmable, and Thermorecyclable Soft Robots, *Adv. Funct. Mater.*, 2021, **31**(32), 2101825, DOI: 10.1002/adfm.202101825.
10 N. Ebrahimi, C. Bi, D. J. Cappelleri, G. Ciuti, A. T. Conn, D. Faivre, N. Habibi, A. Hošovský, V. Iacovacci, I. S. M. Khalil, V. Magdanz, S. Misra, C. Pawashe, R. Rashidifar, P. E. D. Soto-Rodriguez, Z. Fekete and A. Jafari, Magnetic Actuation Methods in Bio/Soft Robotics,

Adv. Funct. Mater., 2021, **31**(11), 2005137, DOI: **10.1002/adfm.202005137**.

11 R. M. Erb, J. J. Martin, R. Soheilian, C. Pan and J. R. Barber, Actuating Soft Matter with Magnetic Torque, *Adv. Funct. Mater.*, 2016, **26**(22), 3859–3880, DOI: **10.1002/adfm.201504699**.

12 X. Zhang, L. Sun, Y. Yu and Y. Zhao, Flexible Ferrofluids: Design and Applications, *Adv. Mater.*, 2019, **31**(51), 1903497, DOI: **10.1002/adma.201903497**.

13 M. Sun, C. Tian, L. Mao, X. Meng, X. Shen, B. Hao, X. Wang, H. Xie and L. Zhang, Reconfigurable Magnetic Slime Robot: Deformation, Adaptability, and Multifunction, *Adv. Funct. Mater.*, 2022, 2112508, DOI: **10.1002/adfm.202112508**.

14 P. Dunne, T. Adachi, A. A. Dev, A. Sorrenti, L. Giacchetti, A. Bonnin, C. Bourdon, P. H. Mangin, J. M. D. Coey, B. Doudin and T. M. Hermans, Liquid Flow and Control without Solid Walls, *Nature*, 2020, **581**(7806), 58–62, DOI: **10.1038/s41586-020-2254-4**.

15 J. Čejková, T. Banno, M. M. Hanczyc and F. Štěpánek, Droplets As Liquid Robots, *Artif. Life*, 2017, **23**(4), 528–549, DOI: **10.1162/ARTL_a_00243**.

16 X. Fan, M. Sun, L. Sun and H. Xie, Ferrofluid Droplets as Liquid Microrobots with Multiple Deformabilities, *Adv. Funct. Mater.*, 2020, **30**(24), 2000138, DOI: **10.1002/adfm.202000138**.

17 W. Yu, H. Lin, Y. Wang, X. He, N. Chen, K. Sun, D. Lo, B. Cheng, C. Yeung, J. Tan, D. Di Carlo and S. Emaminejad, A Ferrobotic System for Automated Microfluidic Logistics, *Sci. Rob.*, 2020, **5**(39), eaba4411, DOI: **10.1126/scirobotics.aba4411**.

18 A. Li, H. Li, Z. Li, Z. Zhao, K. Li, M. Li and Y. Song, Programmable Droplet Manipulation by a Magnetic-Actuated Robot, *Sci. Adv.*, 2020, **6**(7), eaay5808, DOI: **10.1126/sciadv.aay5808**.

19 M. Zhou, Z. Wu, Y. Zhao, Q. Yang, W. Ling, Y. Li, H. Xu, C. Wang and X. Huang, Droplets as Carriers for Flexible Electronic Devices, *Adv. Sci.*, 2019, **6**(24), 1901862, DOI: **10.1002/advs.201901862**.

20 X. Fan, X. Dong, A. C. Karacakol, H. Xie and M. Sitti, Reconfigurable Multifunctional Ferrofluid Droplet Robots, *Proc. Natl. Acad. Sci. U. S. A.*, 2020, **117**(45), 27916–27926, DOI: **10.1073/pnas.2016388117**.

21 J. M. Matxain, J. M. Asua and F. Ruipérez, Design of New Disulfide-Based Organic Compounds for the Improvement of Self-Healing Materials, *Phys. Chem. Chem. Phys.*, 2016, **18**(3), 1758–1770, DOI: **10.1039/C5CP06660C**.

22 X. Kuang, S. Wu, Q. Ze, L. Yue, Y. Jin, S. M. Montgomery, F. Yang, H. J. Qi and R. Zhao, Magnetic Dynamic Polymers for Modular Assembling and Reconfigurable Morphing Architectures, *Adv. Mater.*, 2021, **33**(30), 2102113, DOI: **10.1002/adma.202102113**.

23 Y.-L. Liu and T.-W. Chuo, Self-Healing Polymers Based on Thermally Reversible Diels–Alder Chemistry, *Polym. Chem.*, 2013, **4**(7), 2194–2205, DOI: **10.1039/C2PY20957H**.

24 J. Canadell, H. Goossens and B. Klumperman, Self-Healing Materials Based on Disulfide Links, *Macromolecules*, 2011, **44**(8), 2536–2541, DOI: **10.1021/ma2001492**.

25 Z. Song, Z. Wang and S. Cai, Mechanics of Vitrimer with Hybrid Networks, *Mech. Mater.*, 2021, **153**, 103687, DOI: **10.1016/j.mechmat.2020.103687**.

26 M. Zhang, F. Zhao, W. Xin and Y. Luo, Room-Temperature Self-Healing and Reprocessable Waterborne Polyurethane with Dynamically Exchangeable Disulfide Bonds, *ChemistrySelect*, 2020, **5**(15), 4608–4618, DOI: **10.1002/slct.201904316**.

27 H. Yuk, S. Lin, C. Ma, M. Takaffoli, N. X. Fang and X. Zhao, Hydraulic Hydrogel Actuators and Robots Optically and Sonically Camouflaged in Water, *Nat. Commun.*, 2017, **8**(1), 14230, DOI: **10.1038/ncomms14230**.

28 J. Zhang, O. Onaizah, K. Middleton, L. You and E. Diller, Reliable Grasping of Three-Dimensional Untethered Mobile Magnetic Microgripper for Autonomous Pick-and-Place, *IEEE Rob. Autom. Lett.*, 2017, **2**(2), 835–840, DOI: **10.1109/LRA.2017.2657879**.

29 L. Maffli, S. Rosset, M. Ghilardi, F. Carpi and H. Shea, Ultrafast All-Polymer Electrically Tunable Silicone Lenses, *Adv. Funct. Mater.*, 2015, **25**(11), 1656–1665, DOI: **10.1002/adfm.201403942**.

30 X. Jian, Y. Hu, W. Zhou and L. Xiao, Self-Healing Polyurethane Based on Disulfide Bond and Hydrogen Bond, *Polym. Adv. Technol.*, 2018, **29**(1), 463–469, DOI: **10.1002/pat.4135**.

31 H. F. Gilbert, Protein Modifications Disulfide Bond Formation, *Encyclopedia of Biological Chemistry III*, Elsevier, 2013, pp. 150–153, DOI: **10.1016/B978-0-12-819460-7.00543-0**.

32 N. J. Van Zee and R. Nicolaÿ, Vitrimers: Permanently Crosslinked Polymers with Dynamic Network Topology, *Prog. Polym. Sci.*, 2020, **104**, 101233, DOI: **10.1016/j.progpolymsci.2020.101233**.

33 B. Krishnakumar, R. V. S. P. Sanka, W. H. Binder, V. Parthasarthy, S. Rana and N. Karak, Vitrimers: Associative Dynamic Covalent Adaptive Networks in Thermoset Polymers, *Chem. Eng. J.*, 2020, **385**, 123820, DOI: **10.1016/j.cej.2019.123820**.